**Aalborg Universitet**

**AALBORG UNIVERSITY**

DENMARK

**Reactive Power Strategy of Cascaded Delta-connected STATCOM Under Asymmetrical Voltage Conditions**

He, Zhixing ; Ma, Fujun; Xu, Qianming; Chen, Yandong; Li, Canbing; Li, Mingshen; Guerrero, Josep M.; Luo, An

# Reactive Power Strategy of Cascaded Delta-connected STATCOM Under Asymmetrical Voltage Conditions

Zhixing He, *Student Member*, *IEEE*,  Fujun Ma, *Member*, *IEEE*,  Qianming Xu, *Student Member*, *IEEE*, Yandong Chen, *Member*, *IEEE*, Canbing Li, *Senior Member*, *IEEE*, Mingshen Li, *Student Member*, *IEEE*, Josep M. Guerrero, *Fellow*, *IEEE* and An Luo, *Senior Member*, *IEEE*

*Abstract*—Cascaded static synchronous compensator (STATC-OM) is an effective solution for reactive power support in middle/high voltage conditions, and it has been widely employed to control reactive power in photovoltaic (PV) plants, wind farms, and industrial occasions. In this paper, reactive power control strategy of cascaded delta-connected STATCOM under asymmetrical voltage conditions is investigated. A new phase current reference calculation method is proposed to support reactive power continually under abnormal voltage conditions considering cluster voltage balancing control and phase current limitation. Constrains between voltage and current phasors of STATCOM are deduced. Then, the analytical expressions of phase currents and circulating current references are solved. Therefore, reactive power support and the safe operation of STATCOM can be obtained simultaneously by limiting the peak value of the phase current references. Furthermore, the reactive power support capability of cascaded STATCOM under asymmetrical voltage conditions is explored and compared by combining the proposed references calculation method with the three generalized current references calculation strategies. Finally, simulation and experiment results have been given to verify the theoretical studies.

*Index Terms*—Reactive power control; asymmetrical voltages; circulating current; phase current references; cascaded STATCOM

## I. INTRODUCTION

With the development of power system and renewable energy sources, more and more nonlinear and unbalanced loads, photovoltaic plants and wind turbines are connected to the networks [1]-[3]. The increasing utilization of nonlinear loads and renewable energy sources (RES) causes several power quality problems and brings new challenges to the ancillary services of grid [3],[4]. To deal with these problems, reactive power support is becoming more important and has received much attention due to its capability to control voltage, to improve the reliability of grid, and to enhance the fault ride-through capability of RES especially under grid fault or abnormal conditions [6]-[8].

Various reactive power support devices have been proposed, such as: switched capacitor, static var compensator (SVC), STATCOM and so on [9]-[11]. Among them, STATCOM technology has been widely studied and developed due to its perfect and flexible performance. As in any three-phase grid connected system, STATCOM is also likely to face grid faults and asymmetrical voltages. There are many publications for the conventional two-level STATCOM with a common dc-link. The operation principle and reactive power control method have been illustrated exhaustively in [12]-[13]. With the recent researches on the reactive power control, it demands that STATCOM should provide reactive power continuously under the asymmetrical grid. In [14], a coordination support of positive and negative sequence reactive power was realized at a fix-speed induction generator type wind farm to enhance its fault ride-through capability and reduce torque oscillations. In [15], a cooperation control of reactive power was introduced to correct the deviation in positive sequence voltage and to attenuate negative sequence voltage. To support reactive power continually and to guarantee the injected current is permanently within secure operation limits, different safe current injection strategies for STATCOM were proposed and discussed in [16].

Recently, cascaded H-bridge multilevel converters have been one of the most attractive topologies for STATCOM in middle and high voltage applications due to its advantages such as modularization structure, transformer-less and desirable output performance [17]-[19]. Three-phase STATCOM can be connected in two kinds of typical topologies: star-connected and delta-connected structures [20]. Both of them can regulate grid voltages and support positive and negative sequence reactive power. The three phase clusters of delta-connected STATCOM are rated at line to line voltage of the connected grid, which compared to the star-connected structure, the rated current of the switching devices is lower. The study of this

Z. He, Q. Xu, Y. Chen, C. Li, M. Li, and A. Luo are with the College of Electrical and Information Engineering, Hunan University, Changsha 410082, China (e-mail: hezhixingmail@163.com; hnuxqm@foxmail.com; yandong_chen@hnu.edu.cn; licanbing@gmail.com; cqu.ocean@gmail.com; an_luo@126.com).

J. M. Guerrero is with the Department of Energy Technology, Aalborg University, 9220 Aalborg East, Denmark (e-mail: joz@et.aau.dk).

F. Ma is with the College of Electrical and Information Engineering, Hunan University, Changsha 410082, China (corresponding author, phone: +86-731-88823964; fax: +86-731-88823700; e-mail: mafujun2004@163.com).

paper will focus on delta-connected STATCOM.

Several investigations have been carried out for delta-connected STATCOM. In [21]-[23], reactive power and unbalanced load compensation were illustrated in detail. Voltage balancing control and performance optimization were discussed in [24]-[27]. Two compensation modes of delta-connected STATCOM were discussed in [28], and an individual phase instantaneous current control method was proposed to simplify the compensation method. Circulating current is treated as an extra control freedom of delta-connected STATCOM to transport active powers among three clusters in [29], and a hierarchical voltage control strategy, which includes three cascaded loops, was proposed to regulate capacitor voltages. In this strategy, three proportional and integral (PI) controllers were employed in cluster balancing control loop to synthesize the circulating current reference. STATCOM was utilized to rebalance the unbalanced voltage in [30], while this paper mainly focused on the phase cluster power balancing control. Most studies, however, focused on the unbalanced load compensation and dc-link voltage balancing control. The negative sequence injection capability of cascaded STATCOM was investigated deeply in [31]. The impact of STATCOM on the integration of a large wind farm into weak power system was analyzed in [32]. This research revealed that the grid-side voltage fluctuation caused by uncontrolled resources could be suppressed effectively with reactive power. However, little attention has been paid to the reactive power control of delta-connected STATCOM under asymmetrical voltage conditions. Furthermore, the growing development of RES has led to a change in the requirements of reactive power support services [33]. STATCOM is demanded to support reactive power continuously during asymmetrical grid faults in order to control grid voltages and to enhance fault ride-through capability of RES [34]-[35]. In addition, delta-connected STATCOM exhibited several characteristics compared to conventional two-level converters, and the reactive power control strategies proposed in [14]-[16] are not suitable in this case. Especially, the float dc-link capacitor of each module instead of a common capacitor demanded inner-triangular circulating current to preserve the balancing of capacitor voltages, which will increase the complexity of control method and reduce the reactive power support capacity of STATCOM. Therefore, it is important to investigate the reactive power control method and reactive power support capability of the delta-connected STATCOM under asymmetrical voltage conditions, so as to meet these requirements.

The reactive power control strategy of delta-connected STATCOM under asymmetrical conditions is investigated in this paper. A new reactive current reference calculation method is presented for delta-connected STATCOM to deliver reactive power and to guarantee dc-link voltage balance and phase current within the secure operation limits. Furthermore, the reactive power support capability of cascaded delta-connected STATCOM under abnormal conditions is explored and compared by combining the proposed references calculation method with three generalized current references calculation strategies for conventional two-level converter, namely, active

power oscillation elimination (APOE), reactive power oscillation elimination (RPOE) and balanced positive sequence current injection (BPSC).

This paper is organized as follows. Circulating current and phase currents under asymmetrical conditions are solved in Section II. The reactive current reference calculation method is proposed in Section III. Reactive power support capability of STATCOM is investigated with the three generalized current references calculation methods considering peak phase current limitation in Section IV. Simulation and experiment results are presented to validate the proposed method in Section V. Finally, conclusions are drawn in Section VI.

## II. CIRCULATING CURRENT OF DELTA-CONNECTED STATCOM

Delta-connected STATCOM is depicted in Fig. 1; $i_0$ is the circulating current, $i_a$, $i_b$, $i_c$ are line currents and $i_{ab}$, $i_{bc}$, $i_{ca}$ are phase currents of STATCOM. $Z_g$ is the grid impedance, $v_{ga}$, $v_{gb}$, $v_{gc}$ and $v_a$, $v_b$, $v_c$ are voltages of grid side and point of common coupling (PCC), STATCOM is connected to PCC directly.
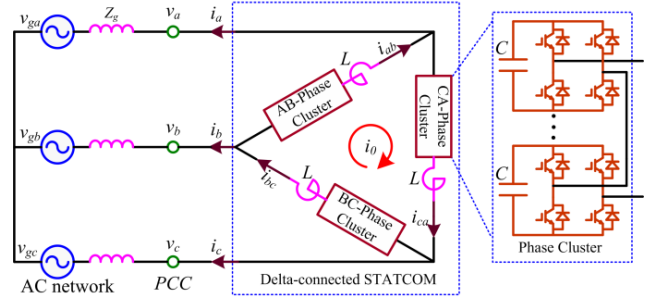


Fig. 1. Schematic configuration of delta-connected STATCOM.

Under asymmetrical voltage conditions, the instantaneous phase voltages at the PCC in Fig. 1 can be expressed as

$$\begin{cases} v_a = V^+ \sin(\omega t) + V^- \sin(\omega t + \theta) \\ v_b = V^+ \sin(\omega t - 2\pi/3) + V^- \sin(\omega t + \theta + 2\pi/3) \\ v_c = V^+ \sin(\omega t + 2\pi/3) + V^- \sin(\omega t + \theta - 2\pi/3) \end{cases} \quad (1)$$

Where $V^+$ is the amplitude of positive sequence voltage, $V^-$ and $\theta$ are the amplitude and phase angle of negative sequence voltage. Applying the $dq$ transformation into (1), the positive and negative sequence voltages at the PCC can be expressed as

$$v_{dq}^+ = v_d^+ + jv_q^+, \ v_{dq}^- = v_d^- + jv_q^- \quad (2)$$

Where $v_{dq}^+$ is the $dq$ components of positive sequence voltage and $v_{dq}^-$ is the $dq$ components of negative sequence voltage. Similarly, the positive and negative sequence currents of line currents in Fig.1 can be expressed as

$$i_{dq}^+ = i_d^+ + ji_q^+, \ i_{dq}^- = i_d^- + ji_q^- \quad (3)$$

Where, $i_{dq}^+$ and $i_{dq}^-$ are the $dq$ components of positive and negative sequence currents. For delta-connected STATCOM, the relationship between line currents and phase currents are expressed as

$$\begin{bmatrix} i_{ab} \\ i_{bc} \\ i_{ca} \end{bmatrix} = \begin{bmatrix} 1/3 & -1/3 & 0 \\ 0 & 1/3 & -1/3 \\ -1/3 & 0 & 1/3 \end{bmatrix} \begin{bmatrix} i_a \\ i_b \\ i_c \end{bmatrix} + \begin{bmatrix} i_0 \\ i_0 \\ i_0 \end{bmatrix} \quad (4)$$
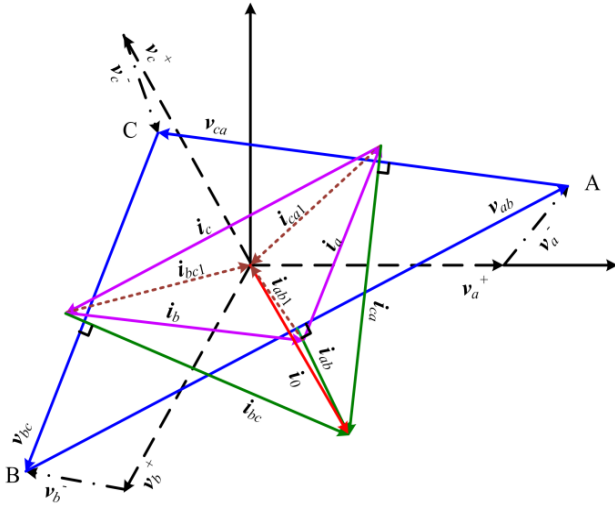
Fig. 2 Phasor diagram of delta-connected STATCOM.

From (4), it can be known that the phase currents are not only determined by line currents but also the circulating current, which is the main difference between delta-connected cascaded and conventional two-level STATCOM.

Unlike the converter with a common dc-link, the dc-link capacitors of cascaded STATCOM are separated and isolated. The dc active power components of three clusters produced by line voltages and phase currents are always unbalanced when STATCOM operates under unbalanced conditions. Circulating current can be employed to redistribute the unbalanced active powers. Phasor analysis is employed in this paper to solve the phase currents and circulating current. Fig.2 shows phasors diagram of delta-connected STATCOM.

In Fig. 2, $v_{ab}$, $v_{bc}$, $v_{ca}$ are the unbalanced line voltage phasors, $i_a$, $i_b$, $i_c$ are the line current phasors, which contain positive and negative sequence reactive components. As shown in Fig. 2, since phasors $i_{ab1}$, $i_{bc1}$, $i_{ca1}$ and line voltage phasors $v_{ab}$, $v_{bc}$, $v_{ca}$ are non-orthogonal, it would lead to that clusters of STATCOM absorb or release active power continuously, as a result, the dc-link voltages diverged. Circulating current could be introduced to rebalance the voltages. According to (4), after adding the circulating current to three phase currents, phase current phasors $i_{ab}$, $i_{bc}$, $i_{ca}$ become orthogonal to the line voltage phasors $v_{ab}$, $v_{bc}$, $v_{ca}$ respectively as shown in Fig. 2.

$$i_{ab} \perp v_{ab}, \; i_{bc} \perp v_{bc}, \; i_{ca} \perp v_{ca} \tag{5}$$

Setting circulating current phasor $i_0$ is

$$i_0 = x + jy \tag{6}$$

If the synchronous signal is determined such that $v_q^+ = 0$ using a phase locked loop [30]. Based on (1) and (2), line voltage phasors can be expressed as

$$
\begin{cases}
v_{ab} = \dfrac{\sqrt{3}}{2}((\sqrt{3}v_d^+ + \sqrt{3}v_d^- + v_q^-) + j(v_d^+ - v_d^- + \sqrt{3}v_q^-)) \\
v_{bc} = \sqrt{3}(-v_q^- + j(-v_d^+ + v_d^-)) \\
v_{ca} = \dfrac{\sqrt{3}}{2}((v_q^- - \sqrt{3}v_d^+ - \sqrt{3}v_d^-) + j(v_d^+ - v_d^- - \sqrt{3}v_q^-))
\end{cases} \tag{7}
$$

Combining (2), (4) and (6), phase current phasors $i_{ab}$, $i_{bc}$, $i_{ca}$ are calculated as follows

$$
\begin{cases}
i_{ab} = (x - \dfrac{i_q^+}{2\sqrt{3}} + \dfrac{i_q^-}{2\sqrt{3}} + \dfrac{i_d^-}{2}) + j(y + \dfrac{i_q^+}{2} + \dfrac{i_q^-}{2} - \dfrac{i_d^-}{2\sqrt{3}}) \\
i_{bc} = (x + \dfrac{\sqrt{3}i_q^+}{3} - \dfrac{\sqrt{3}i_q^-}{3}) + j(y + \dfrac{\sqrt{3}i_d^-}{3}) \\
i_{ca} = (x - \dfrac{i_q^+}{2\sqrt{3}} + \dfrac{i_q^-}{2\sqrt{3}} - \dfrac{i_d^-}{2}) + j(y - \dfrac{i_q^+}{2} - \dfrac{i_q^-}{2} - \dfrac{i_d^-}{2\sqrt{3}})
\end{cases} \tag{8}
$$

Combining (5), (7) and (8), there are

$$
\begin{cases}
x(\sqrt{3}v_d^+ + \sqrt{3}v_d^-) + \sqrt{3}yv_q^- - i_q^+v_d^- + i_q^-v_d^+ = 0 \\
-\sqrt{3}v_q^-x + \sqrt{3}y(v_d^- - v_d^+) - i_q^+v_q^- - i_d^-v_d^+ = 0
\end{cases} \tag{9}
$$

Therefore, the expression of circulating current phasor $i_0$ can be obtained as follows

$$
i_0 = \frac{i_q^+(v_d^-v_d^- - v_d^-v_d^+ - v_q^-v_q^-) + v_d^+i_q^-(v_d^+ - v_d^-) - v_d^+v_q^-i_d^-}{\sqrt{3}(v_d^-v_d^- - v_d^+v_d^+ + v_q^-v_q^-)} +
$$
$$
j\frac{i_q^+(v_d^-v_q^- + v_d^-v_q^- + v_d^+v_q^-) + v_d^+i_d^-(v_d^+ + v_d^-) - v_d^+v_q^-i_q^-}{\sqrt{3}(v_d^-v_d^- - v_d^+v_d^+ + v_q^-v_q^-)} \tag{10}
$$

## III. CURRENT REFERENCES AND REACTIVE POWER CONTROL OF STATCOM UNDER UNBALANCED CONDITIONS

### A. Phase currents and circulating current references

From the basic power theory, the instantaneous active and reactive power under asymmetrical voltage conditions can be calculated as follows [37].

$$
\begin{cases}
p = P_0 + P_{c2}\cos(2\omega t) + P_{s2}\sin(2\omega t) \\
q = Q_0 + Q_{c2}\cos(2\omega t) + Q_{s2}\sin(2\omega t)
\end{cases} \tag{11}
$$

$$
\begin{cases}
P_0 = 1.5(v_d^+i_d^+ + v_q^+i_q^+ + v_d^-i_d^- + v_q^-i_q^-) \\
P_{c2} = 1.5(v_d^-i_d^+ + v_d^+i_d^- + v_q^+i_q^- + v_q^-i_q^+) \\
P_{s2} = 1.5(v_d^-i_d^+ - v_q^-i_q^+ - v_q^+i_q^- + v_d^+i_d^-) \\
Q_0 = 1.5(v_q^+i_d^+ - v_d^+i_q^+ - v_d^-i_q^- + v_q^-i_d^-) \\
Q_{c2} = 1.5(v_d^-i_d^+ - v_q^-i_q^+ + v_q^+i_q^- - v_d^+i_d^-) \\
Q_{s2} = 1.5(v_d^+i_q^- + v_q^+i_d^- - v_q^-i_d^+ - v_d^-i_q^+)
\end{cases} \tag{12}
$$

Where $P_0$ and $Q_0$ are the average values of the instantaneous active and reactive power, $P_{c2}$, $P_{s2}$, $Q_{c2}$, $Q_{s2}$ are the magnitudes of the oscillating terms. Comparing to the reactive power, the average active power $P_0$ is small and can be neglected since it is only utilized to compensate power losses. While, the reactive power $Q_0$ is always controlled to the reactive power reference. Then, the two resting degrees of freedom can be utilized to cancel either the active power oscillation or the reactive power oscillation [38]. Therefore, the line current references can be calculated according to the control target with (12).

In order to eliminate the active power oscillating terms in (12), the last two rows can be neglected since the respective reactive power ones are uncontrolled. The average $P_0$ and $Q_0$ are set to zero and $Q^*$, and the target active power oscillating magnitudes are set to zero $P_{c2} = P_{s2} = 0$, then

$$\begin{cases} i_q^{+*} = \dfrac{-2v_d^+ Q^*}{3((V^+)^2+(V^-)^2)} \\ i_d^{-*} = \dfrac{-2v_q^- Q^*}{3((V^+)^2+(V^-)^2)}, \quad i_q^{-*} = \dfrac{2v_d^- Q^*}{3((V^+)^2+(V^-)^2)} \end{cases} \quad (13)$$

To remove the reactive power oscillating terms in (12), the target reactive power oscillating magnitudes are set to zero $Q_{c2}=Q_{s2}=0$, while the middle two rows are neglected as the active power ones are uncontrolled.

The average $P_0$ and $Q_0$ are also set to zero and $Q^*$, as a result, the line current references in $dq$ frame are obtained as

$$\begin{cases} i_q^{+*} = \dfrac{-2v_d^+ Q^*}{3((V^+)^2-(V^-)^2)} \\ i_d^{-*} = \dfrac{2v_q^- Q^*}{3((V^+)^2-(V^-)^2)}, \quad i_q^{-*} = \dfrac{-2v_d^- Q^*}{3((V^+)^2-(V^-)^2)} \end{cases} \quad (14)$$

In the case of balanced positive sequence current injection, the negative sequence current references are forced to zero $i_d^{-*} = i_q^{-*} = 0$, and both the active and reactive power oscillations are uncontrolled.

The line current references are calculated as

$$\begin{cases} i_q^{+*} = \dfrac{-2v_d^+ Q^*}{3(V^+)^2} \\ i_d^{-*} = 0, \quad i_q^{-*} = 0 \end{cases} \quad (15)$$

Based on (13) to (15), the line current references of STATCOM in these three cases can be combined as follows

$$\begin{cases} i_q^{+*} = \dfrac{-2v_d^+ Q^*}{3((V^+)^2+K(V^-)^2)} \\ i_d^{-*} = \dfrac{-2Kv_q^- Q^*}{3((V^+)^2+K(V^-)^2)}, \quad i_q^{-*} = \dfrac{2Kv_d^- Q^*}{3((V^+)^2+K(V^-)^2)} \end{cases} \quad (16)$$

Where, $K$ is 1, -1 and 0 for the three cases of APOE, RPOE and BPSC respectively.

Inserting (16) into (10) and combining with (1) and (2), the expression of circulating current reference can be modified as

$$i_0^* = \dfrac{Q^*}{3\sqrt{3}V^+(1+Kn^2)}(x_0+jy_0) \quad (17)$$

Where

$$\begin{cases} x_0 = \dfrac{2(1+K)n}{(n^2-1)}(\cos\theta - n\cos^2\theta + n\sin^2\theta) \\ y_0 = \dfrac{-2(1+K)n}{(n^2-1)}(2n\cos\theta\sin\theta + \sin\theta) \end{cases} \quad (18)$$

And $n=V^-/V^+$ is the voltage unbalance factor, which indicates the imbalance amount of power system. According to (17) and (18), it is interesting to find that circulating current reference will become zero when $K$ is -1 in the case of RPOE, while the amplitude of circulating current reference has the largest value when $K$ is 1 in the case of APOE.

Developing (8), (16) and (17), phase current references can be calculated as

$$\begin{cases} i_{ab}^* = \dfrac{Q^*}{3\sqrt{3}V^+(1+Kn^2)}(x_{ab}+jy_{ab}) \\ i_{bc}^* = \dfrac{Q^*}{3\sqrt{3}V^+(1+Kn^2)}(x_{bc}+jy_{bc}) \\ i_{ca}^* = \dfrac{Q^*}{3\sqrt{3}V^+(1+Kn^2)}(x_{ca}+jy_{ca}) \end{cases} \quad (19)$$

Where

$$\begin{cases} x_{ab} = 1+nK\cos\theta - \sqrt{3}nK\sin\theta + x_0 \\ y_{ab} = -\sqrt{3} + \sqrt{3}nK\cos\theta + nK\sin\theta + y_0 \\ x_{bc} = -2 - 2nK\cos\theta + x_0 \\ y_{bc} = -2nK\sin\theta + y_0 \\ x_{ca} = 1+nK\cos\theta + \sqrt{3}nK\sin\theta + x_0 \\ y_{ca} = \sqrt{3} - \sqrt{3}nK\cos\theta + nK\sin\theta + y_0 \end{cases} \quad (20)$$

Generally, the maximum reactive power supplied by STATCOM will decrease under asymmetrical voltage conditions. Furthermore, circulating current is required for delta-connected STATCOM to guarantee capacitor balance, which would increase the required current rating and in turn limit the operational range of the compensator. As a result, the maximum reactive power rating is determined by the maximum value of the phase current amplitudes.

Based on (19) and (20), the amplitudes of phase currents $|i_{ab}|$, $|i_{bc}|$ and $|i_{ca}|$ can be obtained respectively. In fact, to calculate the peak current, only the maximum value of the three current amplitudes should be considered

$$I_{\max} = \max\left\{|i_{ab}|,|i_{bc}|,|i_{ca}|\right\} \quad (21)$$

And it can be obtained as follows

$$I_{\max} = \dfrac{Q^*}{3\sqrt{3}V^+(1+Kn^2)}\max\left\{\sqrt{x_{ab}^2+y_{ab}^2},\sqrt{x_{bc}^2+y_{bc}^2},\sqrt{x_{ca}^2+y_{ca}^2}\right\} \quad (22)$$

Note that the harmonics of voltages and currents will have effect on the proposed control method. Assuming that $k$th harmonic exists in the currents of STATCOM, the harmonic will change the maximum value of the three phase current amplitudes calculated according to (22). Furthermore, if $k$th harmonic exists in the voltages, and the $k$th harmonics of voltages and currents are symmetrical, additional active current components should be introduced in the phase currents in order to keep the total active power balanced; if the $k$th harmonics of voltages and currents are asymmetrical, the instantaneous dc active power produced by $k$th harmonic voltage and current of three branches are unbalanced, additional circulating current should be employed to distribute the unbalanced active power. Both additional active current components and circulating current will change the maximum value of the three phase current amplitudes. Fortunately, the amplitude of harmonic is small compared with the fundamental voltage and current in reactive power support occasion, then, the effect caused by harmonic on the proposed control method is small.

### B. Control of STATCOM

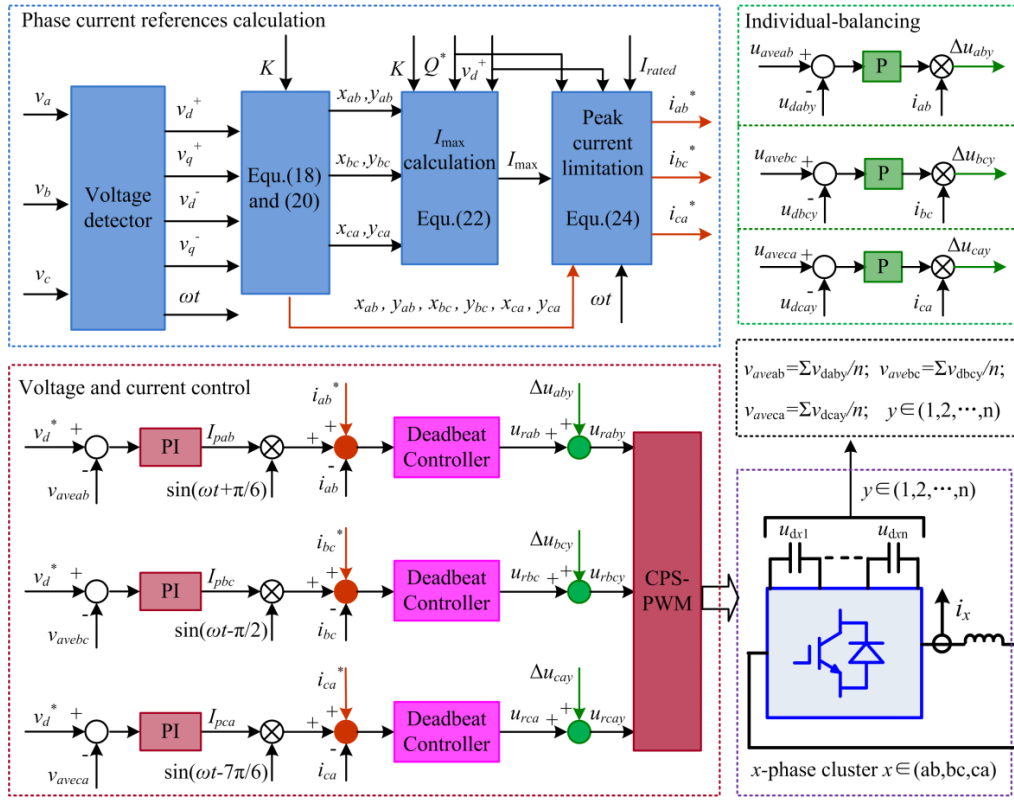Circulating current is employed to keep capacitor voltages

Fig. 3. Diagram of reactive power control strategy with peak current limitation for delta-connected STATCOM

balanced for delta-connected STATCOM under asymmetrical conditions. However, phase currents are no more symmetrical and the maximum reactive power rating is determined by the maximum value of the phase current amplitudes. Therefore, in order to supply reactive power continually and to guarantee a safe operation, a peak current limitation method is quite necessary for STATCOM. Based on the current references calculated in (19), a reactive power control strategy with peak current limitation is presented for delta-connected STATCOM as described in Fig. 3.

Three parts are included in this control strategy: phase current references calculation, individual-balancing control, voltage and current control. The inputs of phase current references calculation are the measured phase voltages $v_a$, $v_b$ and $v_c$ at PCC, the reactive power reference $Q^*$ and $K$, and the rated phase current $I_{rated}$ of STATCOM. Voltage detector based on second-order generalized integrator (SOGI) proposed in [36] is an effective voltage sequence detection method, and it is employed in this paper to detect the grid voltage signals $v_d^+$, $v_q^+$, $v_d^-$, $v_q^-$, and the synchronization signal $\omega t$. $Q^*$ is the reactive power reference for STATCOM, which can be computed according to the voltage control method described in [14] and [15]. According to (18)-(22), the amplitudes of phase current references can be calculated; therefore, the maximum value can be obtained based on (22). Generally, the rated current $I_{rated}$ of STATCOM is a constant, which is determined by circuit elements. If the maximum value of phase current amplitudes is larger than the rated current $I_{max} > I_{rated}$, peak current limitation will be activated to protect STATCOM from over-current. After limited, the peak value of phase current amplitude is reduced and is equal to the rated value. Defining $M$ is a factor to

limit peak current, and $M$ is equal to 1 when $I_{max} \leq I_{rated}$, while $M$ is equal to $I_{rated} / I_{max}$ when $I_{max} \leq I_{rated}$. In this way, the current references shown in (16) can be rewritten as (23)

$$i_q^{+*} = M i_q^{+*}, \; i_d^{-*} = M i_d^{-*}, \; i_q^{-*} = M i_q^{-*} \quad (23)$$

Comparing (16) with (23), line current reference is reduced when the peak current limitation is activated, therefore the reactive power reference is also reduced. Combining (19), (20) and (23), the references of phase current can be calculated as

$$\begin{bmatrix} i_{ab}^* \\ i_{bc}^* \\ i_{ca}^* \end{bmatrix} = \frac{MQ^*}{3\sqrt{3}V^+(1+Kn^2)} \begin{bmatrix} x_{ab} & y_{ab} \\ x_{bc} & y_{bc} \\ x_{ca} & y_{ca} \end{bmatrix} \begin{bmatrix} \sin \omega t \\ \cos \omega t \end{bmatrix} \quad (24)$$

Comparing (19) with (24), it can be concluded that the phase current reference will be reduced if the maximum value of phase current is large than the rated value. It is worth mentioning that circulating current reference shown in (17) is involved in the phase current reference and it can be calculated directly with the instantaneous voltage and control signals to rebalance the unbalanced active power of each cluster.

With the current references solved in (24), the voltage and current control of delta-connected STATCOM is presented in Fig. 3. To keep the average dc-link voltage of each cluster steady, PI controller is adopted. The error between the reference $v_d^*$ and the average voltage $v_{avex}$ of each cluster is regarded as the input of the PI controller, and the output will multiply by the synchronous signal of each line voltage [sin($\omega t$ +π/6+2nπ/3) with n=0,1,2.] to adjust the active component of each phase current. After adding the active power components with the phase current references solved in (24), the final phase current references are obtained. In order to enhance the re-
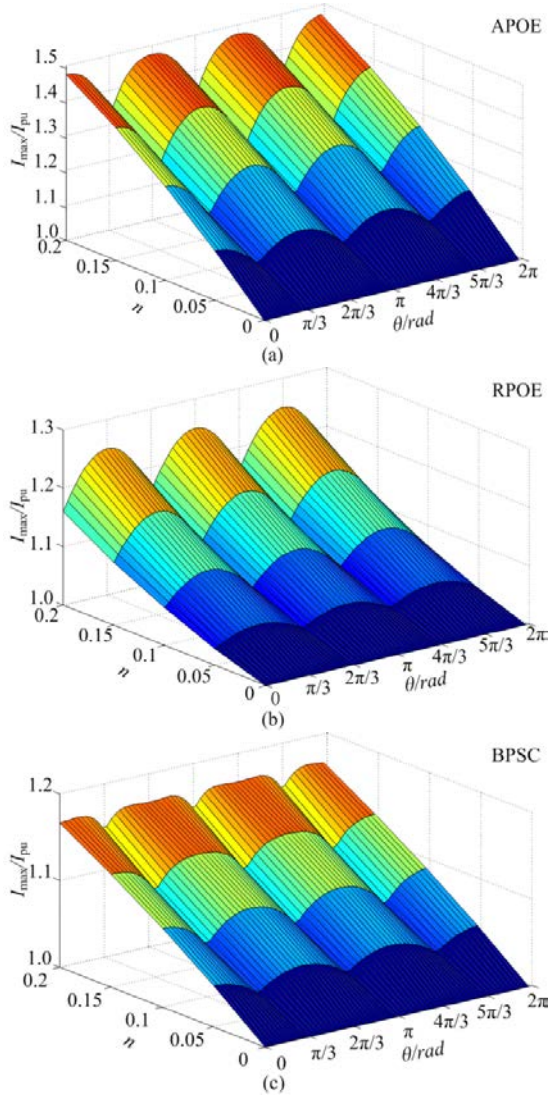
sponse



Fig. 4. Relationship among the maximum current amplitude, unbalanced factor and the phase angle of negative sequence voltage. (a) APOE, (b) RPOE and (c) BPSC.

performance, the deadbeat controller is adopted for the current inner-loop; $v_{rab}$, $v_{rbc}$ and $v_{rca}$ are the modulation signals for the three clusters. Individual balancing control is utilized to regulate capacitor voltage of each H-bridge module in each cluster, and a P controller is used in this control loop. $v_{rxy}$ is the modulation signal of each H-bridge module. Carrier-phase-shifted PWM (CPS-PWM) is also used in this paper. Detailed descriptions of individual balancing control and CPS-PWM are shown in [25] and [28] respectively.

## IV. REACTIVE POWER SUPPORT CAPABILITY OF STATCOM UNDER ASYMMETRICAL CONDITIONS

As shown in Fig. 3, STATCOM could supply reactive power flexibly according to the three generalized current references calculation methods with $K=1$ for APOE, $K=-1$ for RPOE and $K=0$ for BPSC. Since the maximum reactive power decreased under asymmetrical voltage conditions, the three methods APOE, RPOE and BPSC are analyzed and compared taking

peak current limitation into account to investigate the reactive
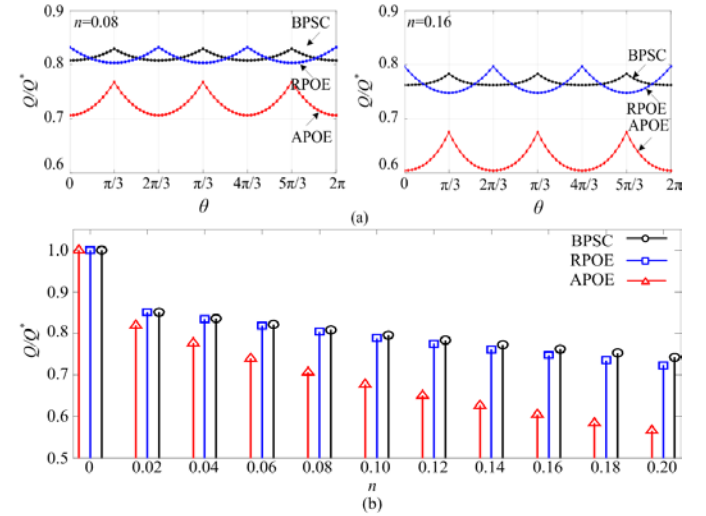


Fig. 5. Relationship among the reactive power rating, unbalanced factor and the phase angle of negative sequence voltage for the three cases: APOE, RPOE and BPSC. (a) reactive power rating of STATCOM when $n$ is 0.08 and 0.16, (b) reactive power rating as a function of the unbalanced factor

power support capability of STATCOM. In the analysis, the maximum current value shown in Fig.4 is calculated according to (20) and (22), and phase current references are calculated from (24) to limit the maximum current value.

From (20) and (22), it is possible to conclude that the maximum current amplitude is sensitive to the voltage unbalance factor $n$ and negative sequence voltage phase angle $\theta$. The relationship between maximum current amplitude, voltage unbalance factor $n$ and phase angle $\theta$ for the three methods are as shown in Fig.4, in which $I_{pu}=Q^*/3\sqrt{3}\ V^+$ is equal to 1 pu. Note that the level of unbalance factor is limited to 0.2 for clarity of the figure. As shown, the worst incidents (i.e., highest demand of the phase current rating) occur when $\theta$ is 0, $2\pi/3$ and $4\pi/3$ for the cases of APOE and BPSC, and $\pi/3$, $\pi$ and $5\pi/3$ for case of RPOE; on the contrary, the lowest demands occur when $\theta$ is $\pi/3$, $\pi$ and $5\pi/3$ for APOE and BPSC, and 0, $2\pi/3$ and $4\pi/3$ for RPOE. From Fig. 4, it is known that APOE has the largest peak current value. Conversely, APOE could provide the least reactive power when the peak phase current is limited to $I_{pu}$. Fig. 5(a) shows the reactive power rating of STATCOM when $n$ is 0.08 and 0.16; BPSC could provide more reactive power; while, RPOE is approximately equal to BPSC when $n$ is 0.08, it is worth mentioning that reactive power rating is also related to $\theta$. Fig. 5(b) shows the reactive power rating as a function of the unbalanced factor considering the worst cases, it is possible to observe that BPSC and RPOE show superior reactive power support performance than APOE when phase current amplitude is limited to the secure value.

As shown in Fig.4 and Fig.5, three methods are analyzed and compared taking peak current limitation into account. The results show that the reactive power rating is related to the voltage unbalance factor $n$ and phase angle $\theta$ of negative sequence voltage. Under asymmetrical voltage conditions, BPSC and RPOE have superior reactive power support capacity than APOE. While, RPOE is similar to BPSC and all depend on $\theta$.

## V.  SIMULATION AND EXPERIMENTAL RESULTS

To evaluate the proposed reactive power control strategy and investigate the impact of unbalanced voltage on reactive power support capability, a delta-connected STATCOM is simulated for a typical photovoltaic plant shown in Fig. 6; STATCOM is connected to 10kV grid directly. Parameters of simulation were listed in Table I.
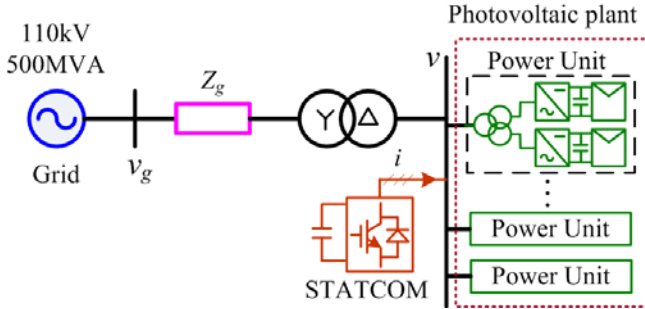


Fig. 6.  Electrical scheme of photovoltaic plants

TABLE I

MAIN PARAMETERS OF SYSTEM

| Parameter | Simulation | Experiment |
|---|---|---|
| The grid line voltage | 110 kV | 0.38 kV |
| Rated voltage of STATCOM | 10 kV, 1 pu | 0.38 kV |
| Rated capacity of STATCOM | 10 Mvar, 1 pu | 24 kvar |
| Rated Current $I_{rated}$ | 472 A | 30 A |
| Cascaded number | 10 | 2 |
| Arm inductance ($L$) | 20 mH | 1 mH |
| SM capacitor ($C$) | 5 mF | 5 mF |
| Carrier frequency ($f_s$) | 200 Hz | 5000 Hz |

Before the grid fault, STATCOM injects 10Mvar reactive power into the balanced grid. To test the effectiveness of the control strategy, 50% voltage amplitude drop is occurred at the high-voltage bus of A-phase at 0.2 s, and the grid voltage is back to be balanced at 0.4s. STATCOM provides reactive power continually during the grid fault and peak current limitation is activated to protect STATCOM without over-passing the rated current $I_{rated}$. The simulation results are shown in Fig.

7. The three cases of APOE, RPOE and BPSC were simulated, and shown in the left, middle and right columns of Fig. 7 respectively. Comparison of the three cases is shown in Table II. The average reactive power supported by STATCOM for the three cases are 0.57pu, 0.79pu and 0.77pu respectively. With reactive power support, line voltages are raised as shown in Table II.

Fig. 7(a) shows the voltages of PCC, since unbalanced grid fault occurred, the voltages become asymmetrical, the THD of voltage is 0.8%. The instantaneous active power and reactive power of STATCOM are shown in Fig. 7(b), it can be seen that the active power oscillation is eliminated during the grid fault in Fig. 7(b) left for APOE, and the reactive power oscillation is eliminated in Fig. 7(b) middle for RPOE, while both active and reactive power have oscillations in Fig. 7(b) right for BPSC. As shown in Table II, RPOE and BPSC supply more average reactive power than APOE; therefore, the amplitude of line voltage is raised higher. It is worth mentioning that the more reactive power STATCOM supplied the higher voltage can be raised, while this paper mainly focused on the operation of STATCOM instead of grid voltage regulation.

Fig. 7(c) shows the line currents of STATCOM, line currents are balanced for BPSC as shown in Fig. 7(c) right, while the others are unbalanced. Note that the STATCOM operated in the safe area all the time. When the maximum value of phase current is larger than the rated current, peak current limitation is activated to protect STATCOM from over-current as shown in Fig. 7(d). The THDs of line currents and phase currents are shown in Table II for the three cases. Fig. 7(e) shows the average capacitor voltages of each cluster. Circulating current reference and circulating current are shown in Fig. 7(f). As the circulating current reference is included in phase current reference, the capacitor voltages of three clusters are kept balanced during the dynamic process.

In order to verify the effectiveness of the proposed strategy, a low voltage experimental prototype of five-level cascaded delta-connected STATCOM was developed. Asymmetrical voltage is made by a 1.1 Ω resistor connected in A-phase and a 30kW three-phase resistance load in this test. In this condition, the voltage unbalanced degree is 8% and THDs of voltage are

TABLE II

COMPARISON OF THREE CURRENT REFERENCE CALCULATION METHODS

| Items | APOE | RPOE | BPSC | $Q^*=0$ |
|---|---|---|---|---|
| Active power $p$ | No Oscillation | Oscillation | Oscillation | / |
| Reactive power $q$ | Oscillation | No Oscillation | Oscillation | / |
| Line currents | Unbalanced | Unbalanced | Balanced | / |
| Average reactive power $Q$ | 0.57pu | 0.79pu | 0.77pu | 0pu |
| Maximum line voltage | 0.94pu | 0.97pu | 0.96pu | 0.92pu |
| Minimum line voltage | 0.68pu | 0.72pu | 0.71pu | 0.65pu |
| THD of $i_a$, $i_b$, $i_c$ (%) | 0.59, 0.61, 0.83 | 0.67, 0.63, 0.53 | 0.67, 0.68, 0.66 | / |
| THD of $i_{ab}$, $i_{bc}$, $i_{ca}$ (%) | 0.85, 1.03, 1.08 | 0.81, 0.93, 1.08 | 0.84, 0.95, 1.01 | / |
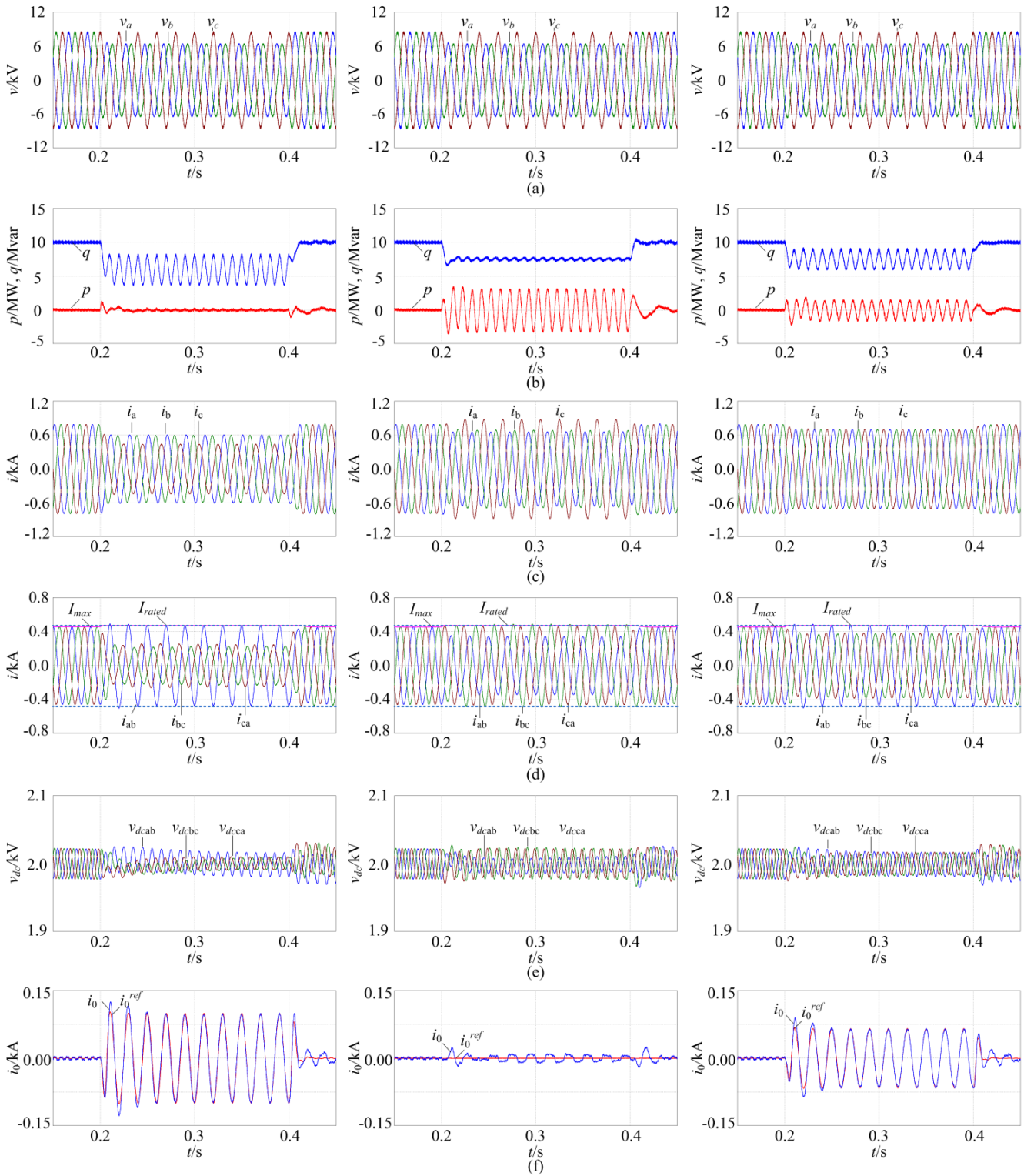
Fig. 7. Simulation results of delta-connected STATCOM. Left: APOE. Middle: RPOE. Right: BPSC. (a) Grid voltages. (b) Active and reactive power. (c) Line currents of STATCOM. (d) Phase currents of STATCOM with peak current limitation. (e) Average capacitor voltages of each cluster. (f) Circulating current.

1.1%, 0.9% and 0.9% for three phases respectively. Parameters of the experiment system are also listed in Table I. The main circuit and controller of the prototype are shown in Fig.8.Two core controllers DSP-TMS320F2812 and FPGA-EP2C8 are utilized in the main board to execute the control algorithm.

Experimental results of the system are shown in Fig. 9. Reactive power reference is set as 24.2kvar in this experiment.

The three cases of APOE, RPOE and BPSC were shown in the left, middle and right columns of Fig. 9 respectively. Fig. 9(a) shows the unbalanced phase voltage in the tests. Instantaneous active and reactive power of the three cases are shown in Fig. 9(b), active power oscillation is eliminated in Fig. 9(b) left, and reactive power oscillation is eliminated in Fig. 9(b) middle; the average reactive power that STATCOM supplied in the three

cases of APOE, RPOE and BPSC are measured as: 18.3kvar, 20.8kvar and 20.3kvar respectively. The experimental results show that RPOE and BPSC supply more average reactive power than APOE, which agrees with the analysis shown in Fig. 5(a). Fig. 9(c) shows line currents of STATCOM, line currents are balanced in the case of BPSC as shown in Fig. 9(c) right, and the others are also unbalanced. As shown in Fig. 9(c) left, $i_a$ has largest amplitude then its THD value is the lowest, THDs of line currents $i_a$, $i_b$ and $i_c$ are 4.6%, 4.8% and 4.9% for APOE. In Fig. 9(c) middle, $i_c$ has largest amplitude and THDs of $i_a$, $i_b$ and $i_c$ are 4.9%, 4.7% and 4.5% for RPOE. Line currents are balanced for BPSC in Fig. 9(c) right, and the THDs are 4.6%,



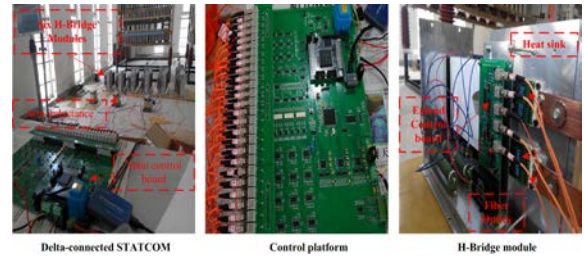Fig. 8. The experimental prototype of delta-connected STATCOM

4.6% and 4.7% respectively. Note that the amplitudes of phase current in the three cases are limited to the rated value when the maximum value of phase current is larger than this value as
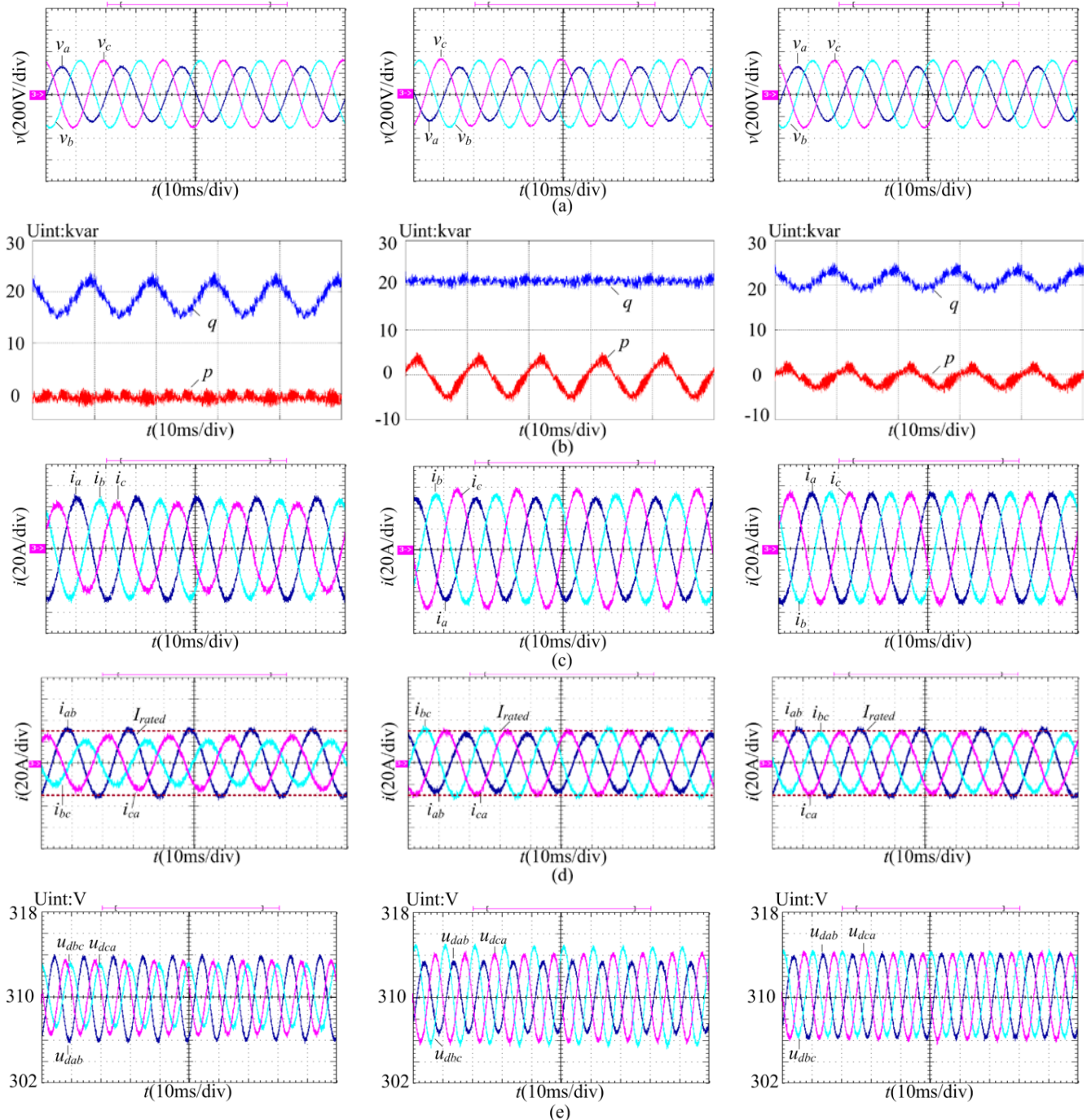


Fig. 9. Experiment results of delta-connected STATCOM. (a) Grid voltages. (b) Active and reactive power. (c) Line currents of STATCOM. (d) Phase currents of

STATCOM with peak current limitation. (e) H-bridge module capacitor voltages of each cluster.
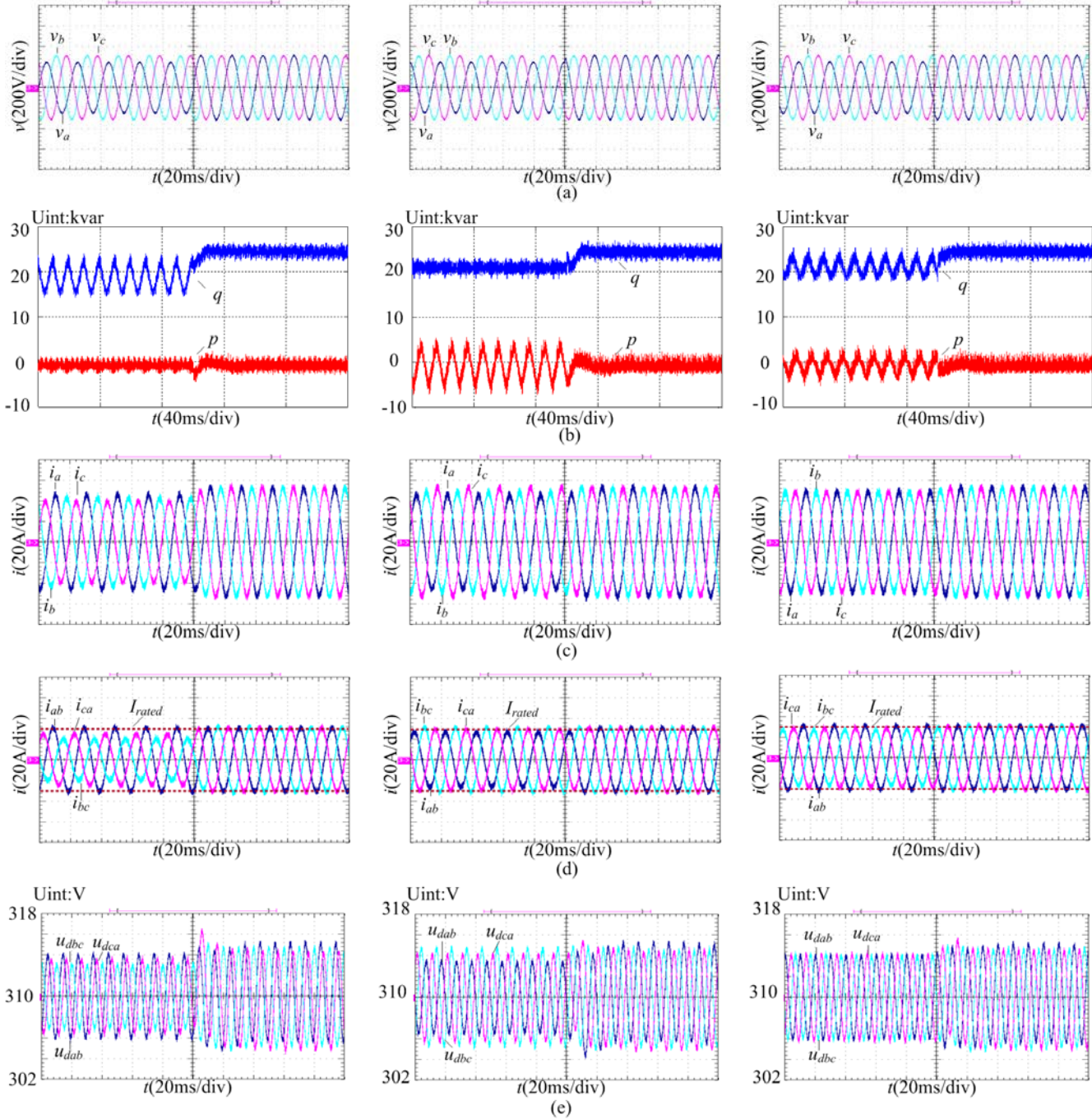


Fig. 10. Dynamic experiment results of delta-connected STATCOM. (a) Grid voltages. (b) Active and reactive power. (c) Line currents of STATCOM. (d) Phase currents of STATCOM with peak current limitation. (e) H-bridge module capacitor voltages of each cluster.

shown in Fig. 9(d), which is very important for the safe operation of STATCOM. THDs of phase currents $i_{ab}$, $i_{bc}$ and $i_{ca}$ are 5.2%, 6.1% and 5.7% for APOE, 6.0%, 5.3% and 5.6% for RPOE, 5.2%, 5.9% and 5.7% for BPSC. Compared Fig. 9(d) with Fig. 9(c), line currents have larger amplitudes in the same case, then THDs of line currents are lower than these of phase currents. Fig. 9(e) shows capacitor voltage of one H-bridge module in each cluster, good voltage balance is obtained.

Dynamic experiment results of the system are shown in Fig. 10. The three cases of APOE, RPOE and BPSC were shown in

the left, middle and right columns of Fig. 10 respectively. During the dynamic process, the 1.1 Ω resistor connected in A-phase is bypassed and the grid voltages are back to be balanced as shown in Fig. 10(a). The performance of STATCOM responding to this dynamic is shown in Fig. 10(b)-(e). The system response is very fast, minor active and reactive power fluctuations occurred and they return normal quickly as shown in Fig. 10(b). Oscillations of active and reactive power are eliminated and reactive power is equal to its references without current limitation when voltages were back to be balanced. Fig.

10(c) and (d) show line currents and phase currents, both of them become balanced. The capacitor voltages are shown in Fig. 10(e), the voltage is controlled to be steady soon after a small voltage step.

## VI. CONCLUSIONS

Reactive power support strategy and capability of cascaded delta-connected STATCOM under asymmetrical voltage conditions are investigated in this paper. Firstly, phase currents and circulating current are solved by analyzing the unbalanced voltages and currents phasors, and then a reactive power support strategy with maximum phase current amplitude limitation is proposed for delta-connected STATCOM. With the proposed method, STATCOM could not only support reactive power continuously but also keep a safe operation all the time, which is important for STATCOM especially under asymmetrical grid fault conditions. Secondly, reactive power support capability of cascaded STATCOM under asymmetrical conditions is investigated based on the proposed method, and the results show that BPSC and RPOE have superior reactive power support capacity than APOE for delta-connected STATCOM under abnormal voltage conditions. Simulation and experiments have been provided to verify the investigations. Since RES could also support reactive power, the future work will focus on the coordinated reactive power control strategy of RES and STATCOM under the abnormal grid.

## REFERENCES

[1] F. Blaabjerg, R. Teodorescu, M. Liserre, and A. V. Timbus, "Overview of control and grid synchronization for distributed power generation systems," *IEEE Trans. Ind. Electron.*, vol. 53, no. 5, pp. 1398-1409, Oct. 2006

[2] S. Kouro, M. Malinowski, K. Gopakumar, J. Pou, L. G. Franquelo, B. Wu J. Rodriguez M. A. Pérez, and J. I. Leon, "Recent Advances and Industrial Applications of Multilevel Converters," *IEEE Trans. Ind. Electron.*, vol. 57, no. 8, pp. 2553-2580, Aug. 2010.

[3] A. Milczarek, M. Malinowski, and J. M. Guerrero, "Reactive Power Management in Islanded Microgrid-Proportional Power Sharing in Hierarchical Droop Control," *IEEE Trans. Smart. Grid.*, vol. 6, no. 4, pp. 1631-1638, Jul. 2015.

[4] S. Kouro, J. I. Leon, D. Vinnikov, and L. G. Franquelo, "Grid-Connected Photovoltaic Systems: An Overview of Recent Research and Emerging PV Converter Technology," *IEEE Industrial Electronics Magazine.*, vol. 9, no. 1, pp. 47-61, March. 2015.

[5] M. Altin, O. Goksu, R. Teodorescu, P. Rodriguez, B.-B. Jensen, and L. Helle, "Overview of recent grid codes for wind power integration," in *Proc. 12th Int. Conf. Optimization Elect. Electron. Equipment*, May 2010, pp. 1152-1160.

[6] P. Rodriguez, A. Timbus, R. Teodorescu, M. Liserre, and F. Blaabjerg, "Reactive power control for improving wind turbine system behavior under grid faults," *IEEE Trans. Power Electron.*, vol. 24, no. 7, pp. 1798-1801, Jul. 2009.

[7] R. G. Wandhare, and V. Agarwal, "Reactive power capacity enhancement of a PV-grid system to increase PV penetration level in smart grid scenario," *IEEE Trans. Smart. Grid.*, vol. 5, no. 4, pp. 1845-1854, Jul. 2014.

[8] F. Wang, J. L. Duarte, and M. A. Hendrix, "Pliant active and reactive power control for grid-interactive converters under unbalanced voltage dips," *IEEE Trans. Power Electron.*, vol. 26, no. 5, pp. 1511-1521, May. 2011.

[9] J. J. Wang, C. Fu, and Y. Zhang, "SVC Control System Based on Instantaneous Reactive Power Theory and Fuzzy PID," *IEEE Trans. Ind. Electron.*, vol. 55, no. 4, pp. 1658-1665, Apr. 2008.

[10] W. L. Chen, W. G. Liang, and H. S. Gau, "Nonlinear Adaptive Volterra Filter for Control of Distribution Static Compensator," *IEEE J. of Emerging and Select. Topics in Power Electron.*, vol. PP, no. 99, pp. 1-1, Dec. 2016.

[11] M. B. Shadmand, M. Mosa, R. S. Balog, and H. Abu-Rub, "Model Predictive Control of a Capacitor-less Matrix Converter Based STATCOM," *IEEE J. of Emerging and Select. Topics in Power Electron.*, vol. PP, no. 99, pp. 1-1, Dec. 2016.

[12] Sabha Raj Arya, and Bhim Singh, "Performance of DSTATCOM Using Leaky LMS Control Algorithm", *IEEE J. of Emerging and Select. Topics in Power Electron.*, vol. 1, no. 2, pp. 104-113, June. 2013.

[13] G. Escobar, A. M. Stanković, and P. Mattavelli, "An adaptive controller in stationary reference frame for D-STATCOM in unbalanced operation," *IEEE Trans. Ind. Electron.*, vol. 51, no. 2, pp. 401-409, Apr. 2004.

[14] C. Wessels, N. Hoffmann, M. Molinas, and F. W. Fuchs, "StatCom control at wind farms with fixed-speed induction generators under asymmetrical grid faults," *IEEE Trans. Ind. Electron.*, vol. 60, no. 7, pp. 2864-2873, Jul. 2013.

[15] M. Castilla, J. Miret, A. Camacho, J. Matas, and Luis. G. de Vicuñal, "Voltage support control strategies for static synchronous compensators under unbalanced voltage sags," *IEEE Trans. Ind. Electron.*, vol. 61, no. 2, pp. 808-820, Feb. 2014.

[16] P. Rodriguez, G. Medeiros, A. Luna, M. C. Cavalcanti, and R. Teodorescu, "Safe current injection strategies for a STATCOM under asymmetrical grid faults," in *Proc. IEEE ECCE*, 2010, pp. 3929-3935.

[17] L. K. Haw, Mohamed S. A. Dahidah, and Haider A. F. Almurib, "A New Reactive Current Reference Algorithm for the STATCOM System Based on Cascaded Multilevel Inverters," *IEEE Trans. Power Electron.*, vol. 8, no. 7, pp. 1312-1328, Jul. 2015.

[18] K. Sano and M. Takasaki, "A Transformerless D-STATCOM Based on a Multivoltage Cascade Converter Requiring No DC Sources," *IEEE Trans. Power Electron.*, vol. 27, no. 6, pp. 2783-2795, June. 2012.

[19] G. Farivar, C. D. Townsend, B. Hredzak, J. Pou and Vassilios G. Agelidis, "Low-Capacitance Cascaded H-Bridge Multilevel StatCom," *IEEE Trans. Power Electron.*, vol. 32, no. 3, pp. 1744-1754, March. 2017.

[20] H. Akagi, "Classification, Terminology, and Application of the modular multilevel cascade converter (MMCC)," *IEEE Trans. Power Electron.*, vol. 26, no. 11, pp. 3119-3130, Nov. 2011.

[21] F. Z. Peng, and J. S. Lai, "Dynamic performance and control of a static var generator using cascade multilevel inverters," *IEEE Trans. Ind. Appl.*, vol. 33, no. 3, pp. 748-755, Oct. 1997.

[22] F. Z. Peng, and J. Wang, "A universal STATCOM with delta-connected cascade multilevel inverter," in the *Annul IEEE Power Electronics Specialists Conference*, Aachen, Germany, pp.3529-3533, 2004.

[23] P. H. Wu, H. C. Chen, Y. T. Chang, and P. T. Chen, "Delta-Connected Cascaded H-bridge Converter Application in Unbalanced Load Compensation," in *IEEE Energy Conversion Congress and Exposition (ECCE),* 2015, pp.6043-6050, Montreal, 20-24 Sept. 2015, Canada.

[24] S. X. Du, J. J. Liu, J. L. Lin, and Y. J. He, "A novel DC voltage control method for STATCOM based on hybrid multilevel H-Bridge converter," *IEEE Trans. Power. Electron.*, vol. 24, no. 1, pp. 45-58, Jan. 2009.

[25] S. Vazquez, J. I. Leon, J. M. Carrasco, L. G. Franquelo, E. Galvan, M. Reyes, J. A. Sanchez, and E. Dominguez, "Analysis of the power balance in the cells of a multilevel cascaded H-Bridge converter," *IEEE Trans. Ind. Electron.*, vol. 57, no. 7, pp. 2287-2296, Jul. 2010.

[26] C. D. Townsend, T. J. Summers, and Robert. E. Betz, "Multigoal Heuristic Model Predictive Control Technique Applied to a Cascaded H-bridge StatCom," *IEEE Trans. Power Electron.*, vol. 27, no. 3, pp. 1191-1200, March. 2012.

[27] R. E. Betz, and T. J. Summers, "Using a cascaded H-bridge STATCOM for rebalancing unbalanced voltages," in *Proc. 7th Int. Conf. Power Electron.*, 2007, pp.1219-1224.

[28] C. Y. Zang, and Z. Liu, "Advanced compensation mode for cascade multilevel static synchronous compensator under unbalanced voltage," *IET. Power. Electron.*, vol.8, Iss. 4, pp. 610-617, Apr. 2015.

[29] M. Hagiwara, R. Maeda, and H. Akagi, "Negative-Sequence reactive-power control by a PWM STATCOM based on a modular multilevel cascade Converter (MMCC-SDBC)," *IEEE Trans. Ind. Appl.*, vol. 48, no. 2, pp. 720-729, Mar. 2012.

[30] R. E. Betz, and T. J. Summers, "Using a cascaded H-bridge STATCOM for rebalancing unbalanced voltages," in *Proc. 7th Int. Conf. Power*

*Electron.*, 2007, pp.1219-1224.

[31] E. Behrouzian, and M. Bongiorno, "Investigation of Negative-Sequence Injection Capability of Cascaded H-Bridge Converters in Star and Delta Configuration," *IEEE Trans. Power. Electron.*, vol. PP, no. 99, pp. 1-1, Jan. 2016.

[32] C, Han, A. Q. Huang, M. E. Baran, S. Bhattacharya, W. Litzenberger, L. Anderson, A. L. Johnson and Abdel-Aty. Edris, "STATCOM Impact Study on the Integration of a Large Wind Farm into a Weak Loop Power System", *IEEE Trans. Energy. Convers.*, vol. 23, no. 1, pp. 226-233, March. 2008.

[33] A. Camacho, M. Castilla, J. Miret, R. Guzman, and A. Borrell, "Reactive Power Control for Distributed Generation Power Plants to Comply With Voltage Limits During Grid Faults," *IEEE Trans. Power. Electron.*, vol. 29, no. 11, pp. 6224-6234, Nov. 2014.

[34] M. Molinas, J. A. Suul, and T. Undeland, "Low Voltage Ride Through of Wind Farms With Cage Generators: STATCOM Versus SVC," *IEEE Trans. Power. Electron.*, vol. 23, no. 3, pp. 1104-1117, May. 2008.

[35] A. M. Shiddiq Yunus, Mohammad A. S. Masoum and A. Abu-Siada, "Effect of STATCOM on the Low-Voltage-Ride-Through Capability of Type-D Wind Turbine Generator," in *Innovative Smart Grid Technology Asia IEEE PES.*, 2011, pp.1-5

[36] P. Rodriguez, J. Pou, J. Bergas, J. I. Candela, R. P. Burgos, and D. Boroyevich, "Decoupled Double Synchronous Reference Frame PLL for Power Converters Control," *IEEE Trans. Power. Electron.*, vol. 22, no. 2, pp. 584-592, March. 2007.

[37] R. Teodorescu, M. Liserre, and P. Rodriguez, *Grid Converters for Photovoltaic and Wind Power Systems*. Hoboken, NJ, USA: Wiley, 2011.

[38] M. Vasiladiotis, N. Cherix, and A. Rufer, "Impact of Grid Asymmetries on the Operation and Capacitive Energy Storage Design of Modular Multilevel Converters," *IEEE Trans. Ind. Electron.*, vol. 62, no. 11, pp. 6697-6707, Nov. 2015.

**Yandong Chen** (M'14) was born in Hunan, China, in 1979. He received the B.S. and M.S. degree in instrument science and technology from Hunan University, Changsha, China, in 2003 and 2006, respectively, and the Ph.D. degree in electrical engineering from Hunan University, Changsha, China, in 2014. He has been an Associate Professor in the College of Electrical and Information Engineering, Hunan University, Changsha.

His research interests include microgrid, power quality, and energy storage. Dr. Chen is a recipient of the 2014 National Technological Invention Awards of China, and the 2014 WIPO-SIPO Award for Chinese Outstanding Patented Invention. He is a member of IEEE Power Electronics Society.

**Canbing Li** (M'06–SM'13) received the B.Eng. and Ph.D. degrees in electrical engineering from Tsinghua University in 2001 and 2006, respectively. He is currently a Full Professor with Hunan University, Changsha, China.

His research interests include smart grid, energy policy, and energy efficiency.

**Mingshen Li** (S'15) received the B.S. degree in electrical engineering from Chongqing University, Chong-qing, China in 2013, and the M.S. degree from Hunan University, Changsha, China, in 2016. He is currently working toward his Ph.D. degree in Aalborg University, Aalborg, Denmark.

His research interests include power quality control, micro-grid and distributed generation systems.

**Zhixing He** (S'15) was born in Hunan, China, 1989. He received the B.S. degree from the College of Information science and Engineering, Central South University, Changsha, China, in 2011. He received the Ph.D. degree in the College of Electrical and Information Engineering, Hunan University, Changsha, China, in 2016. He is currently a Postdoctoral Fellow at Hunan University.

His current research interests include model predictive control, modular multilevel converter, high-frequency link power conversion system.

**Josep M. Guerrero** (FM'15) received the B.S. degree in telecommunications engineering, the M.S. degree in electronics engineering, and the Ph.D. degree in power electronics from the Technical University of Catalonia, Barcelona, in 1997, 2000 and 2003, respectively. Since 2011, he has been a Full Professor with the Department of Energy Technology, Aalborg University, Denmark, where he is responsible for the Microgrid Research Program. From 2012 he is a guest Professor at the Chinese Academy of Science and the Nanjing University of Aeronautics and Astronautics; from 2014 he is chair Professor in Shandong University; from 2015 he is a distinguished guest Professor in Hunan University; and from 2016 he is a visiting professor fellow at Aston University, UK, and a guest Professor at the Nanjing University of Posts and Telecommunications.

**Fujun Ma** (M'15) was born in Hunan, China, 1985. He received the B.S. degree in Automation and Ph.D. degree in Electrical Engineering from Hunan University, Changsha, in 2008 and 2015, respectively.

Since 2013, he has been an Associate Professor with the College of Electrical and Information Engineering, Hunan University. His research interests include power quality managing technique of electrified railway, electric power saving, reactive power compensation, and active power filters.

**Qianming Xu** (S'15) was born in Henan, China, 1989. He received the B.S. degree in Electrical Engineering and Automation from the College of Electrical and Information Engineering, Hunan University, Changsha, China, in 2012. He has been working toward the Ph.D. degree in Electrical Engineering in the College of Electrical and Information Engineering, Hunan University, Changsha since 2012.

His research interests include multilevel converters, power quality control, electric drive and power conversion control.

**An Luo** (SM'09) was born in Changsha, China, in 1957. He received the Ph.D. degree in fluid power transmission and control from Zhejiang University, Hangzhou, China, in 1993. Between 1996 and 2002, he was a Professor with Central South University. Since 2003, he has been a Professor in the College of Electrical and Information Engineering, Hunan University, where he also serves as the Chief of National Electric Power Conversion and Control Engineering Technology Research Center.

His research interests mainly include multilevel converters, microgrid, and power quality. He was elected to the Chinese National Academy of Engineering

(CNAE) in 2015, the highest honor for scientists and engineers and scientists in China. He has won the highly prestigious China National Science and Tech-nology Awards three times (2014, 2010 and 2006).